Error analysis in the electron temperature measurements in TCABR

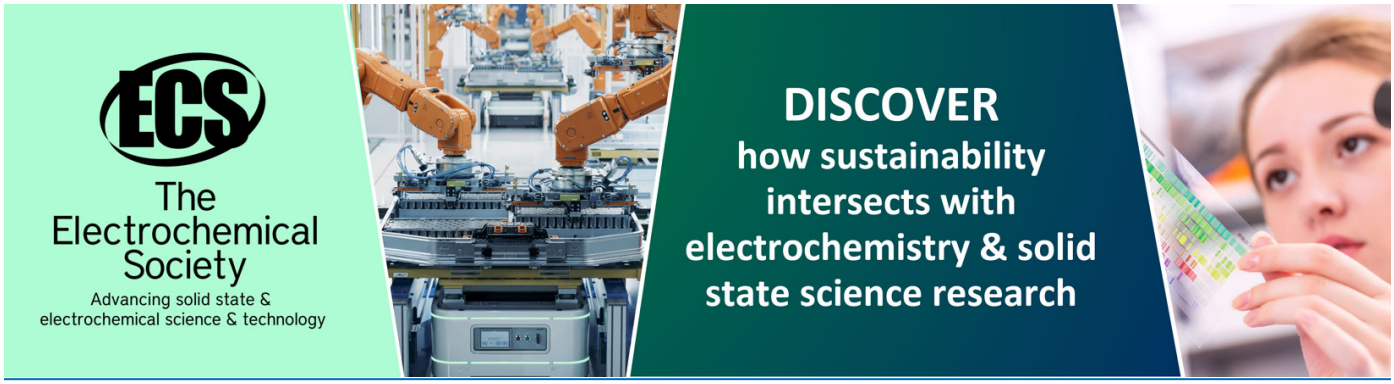

Journal of Physics: Conference Series **370** (2012) 012045 doi:10.1088/1742-6596/370/1/012045

Error analysis in the electron temperature measurements in TCABR

J H F Severo[1], F O Borges[2], M P Alonso[3], R M O Galvão[1], V C Theodoro[1], L A Berni[4], L C Jeronimo[1], J I Elizondo[1], A C A Figueiredo[3], M Machida[5], I C Nascimento[1], Yu K Kuznetsov[1], E K Sanada[1], O C Usuriaga[1] and M Tendler[6]

[1] Institute of Physics, University of São Paulo, Rua do Matão, s/n, 05508-900 SP, Brazil.
[2] Laboratório de Plasma e Espectroscopia Atômica, Instituto de Física, Universidade Federal Fluminense (UFF), 24210-340, Niterói, RJ, Brazil.
[3] Instituto de Plasmas e Fusão Nuclear, Instituto Superior Técnico, Associação Euratom/IST 1049-001, Lisboa, Portugal.
[4] Laboratório Associado de Sensores e Materiais, INPE, 12227-010, São José dos Campos, SP, Brazil.
[5] Universidade Estadual de Campinas, 13083-970 Campinas, SP, Brazil.
[6] Royal Inst Technol, Alfven Lab, Stockholm, Sweden.

E-mail: jhsevero@if.usp.br

Abstract. An analytical method is proposed to evaluate the experimental uncertainty in the electron temperature measurements in the TCABR tokamak. Solving the integral equation resulting from the convolution of two functions, one representing, the scattered light and the other the spectral apparatus function, i.e., the polychromator, an analytical expression for the electron temperature is obtained, from which the uncertainty in the measured value is readily evaluated. The results show that the major contribution to the error comes from the noise in the signal; the uncertainties in the filters parameters do not contribute significantly to the total error.

1. Introduction

The TCABR tokamak is a machine with a broad research program on the physics of magnetically confined plasmas; in particular the interaction of RF waves in the region of Alfvén frequencies [1], stochastic processes at the plasma edge, transport barriers [2-3], plasma rotation [4-6], MHD activity [7], and diagnostic development [8-9]. The Thomson scattering system of TCABR [10] has been developed under a scientific collaboration between the University of São Paulo (Brazil) and the Instituto Superior Técnico (Lisbon, Portugal).

Thomson scattering is the most straightforward and widely used diagnostic in controlled thermonuclear research to measure the electron temperature and density. It was first applied to measure the electron temperature in a tokamak in 1969 by a British-Soviet team [11-12] and thereafter it became a standard technique.

In the Thomson diagnostic, the electron temperature is obtained from the shape of the spectrum $s(\lambda)$ of the scattered light, where λ is the wavelength. However, any apparatus used to measure the spectrum distribution introduces distortions in the spectrum, which have to

be properly taken into account. Mathematically, this distortion can be computed from the convolution of the apparatus function $a(\lambda)$ with the spectral distribution of scattered light, i.e. [13],

$$f(\lambda) = \int_{-\infty}^{+\infty} s(\lambda')a(\lambda - \lambda')d\lambda'. \quad (1)$$

The Thomson Scattering system of TCABR is composed of a vertically oriented Nd:Glass laser beam ($\lambda_i = 1054nm$), a polychromator equipped with three interference filters coupled to silicon APDs (avalanche photodiodes), and a telescope that collimates the scattered light into an optical fiber that transmits this light to the polychromator [8].

Solving (1) for the different interference filters and taking the ratio of the corresponding solutions, an analytical expression for the electron temperature is obtained from which the uncertainty in the measurement can be calculated.

The remainder of this paper is organized as follows. The experimental setup is described in section 2. In section 3, a general expression for electron temperature as a function of signal ratio is derived. The results and discussions are presented in section 4. Section 5 contains the conclusions. Appendix A is dedicated to the evaluation of the uncertainties.

2. Experimental setup

A schematic representation of the Thomson scattering diagnostic of the TCABR tokamak ($R = 0.61m$, $a = 0.18m$) is shown in figure 1. The Nd:Glass laser is Q-switched by a Pockels cell triggered to deliver one pulse per tokamak shot. The plasma volume is probed by the laser beam ($\lambda_i = 1054nm$) in the vertical direction. The scattered light is collected from an $18mm$ long chord localized at the plasma center by an objective lens and transmitted to the polychromator by an optical fiber. The polychromator is composed of band-pass interference filters, to split the light into three spectral bands coupled to three APDs. The detectors integrate the scattered light in three different spectral intervals corresponding to pass-bands of the interference filters. The relative responses of the three polychromator channels are shown in the figure 2. These curves were obtained after calibration and include all system parameters, such as interference filters transmittance, detector quantum efficiency, amplifier gain, etc.. Figure 2 shows also the spectral distribution of the scattered light for an electron temperature of $500eV$ [14].

The transmittance of the filters is approximately 75% and the APDs (RCA type CA30956E) have a quantum efficiency of $85-40\%$ in the range $800-1060nm$. These specifications guarantee the high spectral sensitivity of the diagnostic.

The plasma temperature is evaluated from the signal ratio of polychromator channels, $R = P_{S,i}/P_{S,j}$, where $P_{S,i}$ is the scattered power detected by the $i-th$ channel of the polychromator. This method eliminates the dependence on the power of the incident laser, solid angle, plasma density, spectral response of detector etc. leaving only the dependence on the electron temperature.

3. Electron temperature as function of signal ratio

The theory of Thomson scattering is well described in the literature, and its application to fusion plasmas has been analyzed in detail [15]. According to this reference, as the laser beam propagates through the plasma the power P_S scattered into the wavelength range $\lambda_1 - \lambda_2$ by free electrons within the solid angle of observation $\Delta\Omega$ is given by

$$P_S = P_0 r_0^2 n_e \Delta L \Delta\Omega \int_{\lambda_1}^{\lambda_2} f(\lambda, T_e)\, d\lambda, \quad (2)$$

where P_0 is the power of the incident laser, with wavelength λ_I, r_0 is the classical electron radius, n_e is the plasma density, ΔL is the length of the scattering region as observed by

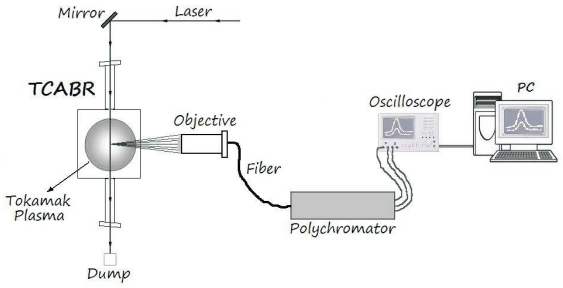

Figure 1. Schematic representation of the experimental arrangement of the Thomson scattering system in the TCABR tokamak.

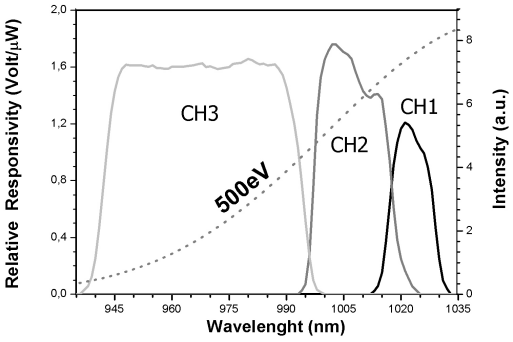

Figure 2. Electron temperature as function of signal ratio.

the collection optics (18 mm in the TCABR). The function $f(\lambda, T_e)$ is given by (1). The function $a(\lambda)$ is sometimes called the transfer function and includes all possible changes in the amplitude and phase of the signal related to the detector characteristics, as quantum efficiency, circuit characteristics, amplifier gain, distortions of the input signals due to diffraction on the diaphragms of the optical system of the spectral apparatus, its aberrations, the finite aperture widths, the time lag of the recording instrument etc., as schematically represented in figure 3.

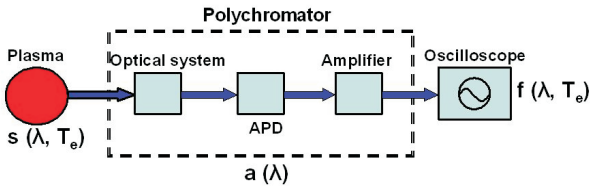

Figure 3. Schematic representation of signal transformation during the measurements process.

The function $s(\lambda, T_e)$ in equation (1) is well described in the literature and has the following form [15]:

$$s(\lambda, T_e) = \frac{1}{\Delta\lambda_e \lambda_I \sqrt{\pi}} \left(\lambda_I - 3.5(\lambda - \lambda_I) + \frac{(\lambda - \lambda_I)^3}{\Delta\lambda_e^2} \right) \exp\left[-\frac{(\lambda - \lambda_I)^2}{\Delta\lambda_e^2} \right], \tag{3}$$

where $\Delta\lambda_e = \frac{2V_T\lambda_I}{c}\sin\left(\frac{\theta}{2}\right)$, c is the speed of light, $V_T = \sqrt{\frac{2K_BT_e}{m_e}}$ is the electron thermal velocity, T_e the electron temperature, k_B the Boltzmann constant, m_e the electron mass, and θ is the observation angle between the electrical field of the incident radiation and the scattering direction.

To evaluate the uncertainty in electron temperature, it is necessary to first obtain an expression for the electron temperature as function of all system parameters e.g., the integral in (1) has to be carried out, inserted into (2), and the resulting integral inverted to explicitly obtain an expression for the electron temperature.

One difficulty with this procedure is that the apparatus function $a(\lambda)$, which is obtained through a calibration process, is known only numerically, as shown in figure 2 for the three interference filters of the TCABR Thomson scattering system. However, considering the global shape of the calibration curves, one realizes that they can be represented as sum of Gaussians, i.e.,

$$a(\lambda) = \sum_{i=1}^{n=3} \sum_{j=1}^{m} g_{i,j}(\lambda) \tag{4}$$

where $g_{i,j}(\lambda) = 1/(\sigma_{i,j}\sqrt{2\pi}) \exp\left[-0.5(\lambda - \lambda_{0,i,j})^2/\sigma_{i,j}^2\right]$, n is the number of interference filters used in the diagnostic, and m is the number of Gaussian functions used to adjust the spectral dependence of each interference filter curve.

A general method to carry out the integration in (1) is based upon using the Fourier transforms of the two functions in the integrand,

$$s(\lambda) = \frac{1}{\sqrt{2\pi}} \int_{-\infty}^{+\infty} S(\omega) e^{i\omega\lambda} d\omega; \qquad a(\lambda) = \frac{1}{\sqrt{2\pi}} \int_{-\infty}^{+\infty} A(\omega) e^{i\omega\lambda} d\omega. \tag{5}$$

Then, (1) can be rewritten as

$$f(\lambda) = \frac{1}{2\pi} \int_{-\infty}^{+\infty} S(\omega) A(\omega) e^{i\omega\lambda} d\omega, \tag{6}$$

where

$$A(\omega) = \frac{1}{\sqrt{2\pi}} \int_{-\infty}^{+\infty} a(\lambda) e^{-i\omega\lambda} d\lambda = \frac{1}{\sqrt{2\pi}} \int_{-\infty}^{+\infty} \sum_{i=1}^{n} \sum_{j=1}^{m} g_{i,j}(\lambda) e^{-i\omega\lambda} d\lambda, \tag{7}$$

is the Fourier transform of the apparatus function. Using the Gaussian expression given by (4), it follows that

$$A(\omega) = \sum_{i=1}^{n} \sum_{j=1}^{m} G_{i,j}(\omega) \qquad G_{i,j}(\omega) = \exp\left[-\left(i\lambda_{0,i,j}\omega + \frac{\omega^2\sigma_{i,j}^2}{2}\right)\right]. \tag{8}$$

Equation (6) can be rewritten in the following way

$$f(\lambda) = \frac{1}{2\pi} \int_{-\infty}^{+\infty} \left[A(\omega) - 1 + 1\right] S(\omega) e^{i\omega\lambda} d\omega,$$

that is,

$$f(\lambda) = \frac{1}{2\pi} \int_{-\infty}^{+\infty} \left[A(\omega) - 1\right] S(\omega) e^{i\omega\lambda} d\omega + s(\lambda). \tag{9}$$

Substituting equation (8) into (9) yields

$$f(\lambda) = \frac{1}{2\pi} \sum_{i=1}^{n} \sum_{j=1}^{m} \int_{-\infty}^{+\infty} \left[G_{i,j}(\omega) - 1\right] S(\omega) e^{i\omega\lambda} d\omega + s(\lambda). \tag{10}$$

The term in brackets in this equation is very small and vanishes in the case of ideal spectral apparatus. In most practical cases, when the half-width of the scattered spectral distribution of light is much wider than the half-width from instrumental broadening, the distortion caused by the real apparatus is very small and this term can be neglect. So, expanding the Fourier transform of the Gaussian function in a Taylor series and substituting in (10) yields

$$f(\lambda) \simeq \frac{1}{2\pi}\sum_{i=1}^{n}\sum_{j=1}^{m}\int_{-\infty}^{+\infty}\left[-i\omega\lambda_{0,i,j} - \frac{1}{2}\omega^2\left(\sigma_{i,j}^2 + \lambda_{0,i,j}^2\right)\right]S(\omega)e^{i\omega\lambda}d\omega + s(\lambda). \tag{11}$$

Taking into account that

$$\frac{ds\left(\lambda\right)}{d\lambda} = \frac{1}{2\pi}\int_{-\infty}^{+\infty} i\omega S(\omega)e^{i\omega\lambda}d\omega \qquad \text{and} \qquad \frac{d^2s\left(\lambda\right)}{d\lambda^2} = -\frac{1}{2\pi}\int_{-\infty}^{+\infty}\omega^2 S(\omega)e^{i\omega\lambda}d\omega,$$

it follows that,

$$f(\lambda) \simeq s(\lambda) - \sum_{i=1}^{n}\sum_{j=1}^{m}\lambda_{0,i,j}\frac{ds\left(\lambda\right)}{d\lambda} + \frac{1}{2}\sum_{i=1}^{n}\sum_{j=1}^{m}\left(\sigma_{i,j}^2 + \lambda_{0,i,j}^2\right)\frac{d^2s\left(\lambda\right)}{d\lambda^2}. \tag{12}$$

The function $s(\lambda)$ has a Gaussian shape for temperatures below $500eV$. The second and third terms in parentheses in (3) are responsible for the relativistic corrections and can be neglected for temperatures below $500eV$. Therefore the function $s(\lambda)$ can be approximately expressed in the following form:

$$s\left(\lambda\right) \simeq \frac{1}{\Delta\lambda_e\sqrt{\pi}}\exp\left[-\frac{\left(\lambda-\lambda_I\right)^2}{\Delta\lambda_e^2}\right], \tag{13}$$

where $\Delta\lambda_e = 2\sqrt{2K_BT_e/m_e}\lambda_I\sin^2\left(\theta/2\right)/c$ and λ_I is wavelength of the incident beam.

Using these results, it follows that the scattered power $P_{S,i}$ measured in each channel is given by

$$P_{S,i} = E_0\left[\int_{\lambda_{1,i}}^{\lambda_{2,i}} s(\lambda)d\lambda - \sum_{j=1}^{m}\lambda_{0,i,j}\int_{\lambda_{1,i}}^{\lambda_{2,i}}\frac{ds\left(\lambda\right)}{d\lambda}d\lambda + \frac{1}{2}\sum_{j=1}^{m}\left(\sigma_{i,j}^2 + \lambda_{0,i,j}^2\right)\int_{\lambda_{1,i}}^{\lambda_{2,i}}\frac{d^2s\left(\lambda\right)}{d\lambda^2}d\lambda\right], \tag{14}$$

where $E_0 = P_0r_0^2n_e\Delta L\Delta\Omega$.

Expanding the function $s(\lambda)$ in a Taylor series around $\lambda = \lambda_{C,i}$ where $\lambda_{C,i}$ represents the central wavelength of $i-th$ interference filter, the power $P_{S,i}$ for each channel can be written as

$$P_{S,i} \simeq \frac{P_0r_0^2n_e\Delta L\Delta\Omega W_ib_i}{\Delta\lambda_e^3\sqrt{2\pi}}\exp\left[-\frac{\left(\lambda_{C,i}-\lambda_I\right)^2}{2\Delta\lambda_e^2}\right]\left(\frac{a_i}{W_ib_i}\Delta\lambda_e^2 + 1\right) \tag{15}$$

where:

$$a_i = W_i - \sum_{j=1}^{m}\lambda_{0,i,j}$$

and

$$b_i = \left[\frac{W_i^2}{24} + \left(\lambda_{C,i}-\lambda_I\right)\sum_{j=1}^{m}\lambda_{0,i,j} - \frac{1}{2}\sum_{j=1}^{m}\left(\sigma_{i,j}^2 + \lambda_{i,j}^2\right)\right]$$

Let $R = P_{S,2}/P_{S,1}$ express the signal ratio between channels 2 and 1, which is a function of the electron temperature and the filters parameters, such as the central wavelength $\lambda_{C,i}$ and the waveband W_i , etc.. Solving this equation with respect to T_e yields,

$$T_e = \frac{-K_1 \pm \sqrt{K_1^2 - 4K_2K_0}}{2K_2}, \tag{16}$$

where:

$$K_2 = A\left(\frac{\lambda_I^2 2k_B}{c^2 m_e}\right)^2,$$
$$K_1 = B\left(\frac{\lambda_I^2 2k_B}{c^2 m_e}\right),$$
$$K_0 = C,$$

and

$$A = 2\left(a_1 W_2 b_2 - a_2 W_1 b_1\right),$$
$$B = 2W_1 W_2 b_1 b_2 \ln\left(\frac{R W_1 b_1}{W_2 b_2}\right),$$
$$C = W_1 W_2 b_1 b_2 \left[\left(\lambda_{C,2} - \lambda_I\right)^2 - \left(\lambda_{C,1} - \lambda_I\right)^2\right].$$

Let now $R = \left(P_{S,3} + P_{S,2}\right)/P_{S,1}$, in this case the electron temperature can be expressed as:

$$T_e = \frac{-K_1 \pm \sqrt{K_1^2 - 4K_2 K_0}}{2K_2}, \tag{17}$$

where:

$$K_2 = A\left(\frac{\lambda_I^2 2k_B}{c^2 m_e}\right)^2,$$
$$K_1 = B\left(\frac{\lambda_I^2 2k_B}{c^2 m_e}\right),$$
$$K_0 = C,$$

$$A = 2\left[a_1\left(W_2 b_2 + W_3 b_3\right) - W_1 b_1\left(a_2 + a_3\right)\right],$$
$$B = 2W_1 b_1\left(W_2 b_2 + W_3 b_3\right) \ln\left(\frac{R W_1 b_1}{W_2 b_2 + W_3 b_3}\right),$$
$$C = W_1 b_1\left(W_2 b_2 + W_3 b_3\right)\left[\left(\lambda_M - \lambda_I\right)^2 - \left(\lambda_{C,1} - \lambda_I\right)^2\right],$$

and

$$\lambda_M = \frac{\lambda_{C,2} W_2 + \lambda_{C,3} W_3}{W_2 + W_3}.$$

4. Results and discussions

The plasma temperature in the TCABR tokamak is evaluated from the signal ratios of the different polychromator channels. Equation (16) gives the electron temperature as a function of the signal ratio between channels 2 and 1, while equation (17) gives the electron temperature as a function of the signal ratio of channel 2 plus channel 3 and channel 1. For the ratio between channels 3 and 1 all indexes 2 in equation (16) should be changed to index 3. These equations show the dependence of electron temperature on the signal ratio and the filters parameters, such as $\lambda_{C,i}$, W_i, $\lambda_{0,i,j}$ and $\sigma_{i,j}$ that are obtained after fitting the curves in figure 2 with a least squares method.

Table 1 gives the central wavelength $\lambda_{0,i,j}$ and bandwidth $\sigma_{i,j}$ of each Gaussian used in equation (4) to express the apparatus function.

Once all parameters in equations (16) and (17) have been obtained, after fitting the curves in figure 2, the dependence of electron temperature on the signal ratio can be calculated. The ratios $R = (P_{S,3} + P_{S,2})/P_{S,1}$ and $R = P_{S,3}/P_{S,1}$ as function of T_e $[eV]$ are shown in figures 4 and 5, respectively. In these figures is also shown the dependence of electron temperature on the signal ratio obtained by computation. The solid line shows the computed results while the dashed line shows the calculated results from equation (16) and (17).

Table 1. Table of parameters obtained by least squares fitting of the curves 1, 2 and 3 in figure 2.

Curve 1 in figure 2	
$\lambda_{0,1,j}$ $[nm]$	$\sigma_{1,j}$ $[nm]$
1019.15 ± 0.03	3.52 ± 0.09
1023.02 ± 0.08	5.93 ± 0.13
1028.17 ± 0.03	3.87 ± 0.04
Curve 2 in figure 2	
$\lambda_{0,2,j}$ $[nm]$	$\sigma_{2,j}$ $[nm]$
999.21 ± 0.09	2.70 ± 0.20
1001.8 ± 0.8	4.4 ± 0.6
1006.2 ± 0.3	6 ± 3
1012.7 ± 0.6	$(90 \pm 13) \cdot 10^{-1}$
1016.43 ± 0.14	3.5 ± 0.6
Curve 3 in figure 2	
$\lambda_{0,3,j}$ $[nm]$	$\sigma_{3,j}$ $[nm]$
945.2 ± 0.3	5.0 ± 0.8
$(9491 \pm 17) \cdot 10^{-1}$	7 ± 4
$(9556 \pm 22) \cdot 10^{-1}$	11 ± 9
$(9689 \pm 21) \cdot 10^{-1}$	17 ± 12
983.1 ± 0.9	11 ± 5
990.1 ± 0.3	$(64 \pm 13) \cdot 10^{-1}$
994.06 ± 0.15	$(23 \pm 12) \cdot 10^{-1}$

The disagreement that occurs for $T_e > 600eV$ in both figures is related to the spectral distribution of the scattered light $s(\lambda)$, which we take as pure Gaussian (equation (13)), and relativistic corrections are not being taken in to account, since the electron temperature in the TCABR tokamak is $< 600eV$.

From the analytical expression for the electron temperature given by equations (16) and (17), the uncertainty in the electron temperature can be calculated by applying the standard method

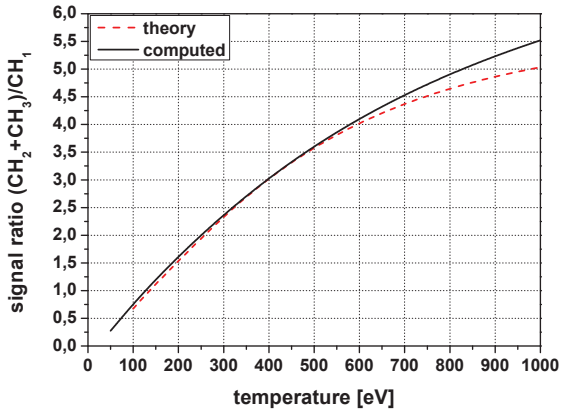

Figure 4. The solid line shows the computed results of $R = (P_{S,3} + P_{S,2})/P_{S,1}$, and the dashed line shows the calculated results from equation (16) and (17).

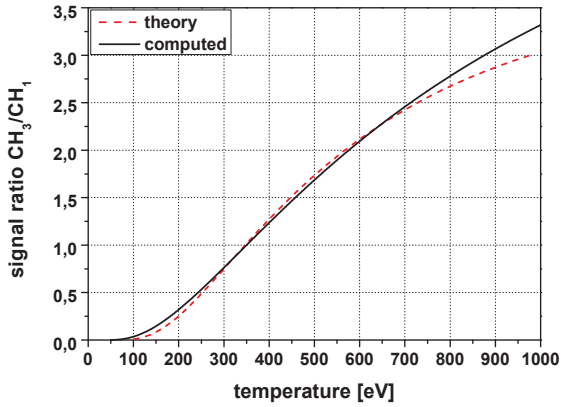

Figure 5. The solid line shows the computed results of $R = P_{S,3}/P_{S,1}$, and the dashed line shows the calculated results from equation (16) and (17).

of error propagation. The standard deviation $\sigma^2_{T_e}$ is given by,

$$\sigma^2_{T_e} = \left(\frac{\partial T_e}{\partial R}\right)^2 \sigma^2_R + \left(\frac{\partial T_e}{\partial \lambda_{C,1}}\right)^2 \sigma^2_{\lambda_{C,1}} + \left(\frac{\partial T_e}{\partial \lambda_{C,2}}\right)^2 \sigma^2_{\lambda_{C,2}} + \left(\frac{\partial T_e}{\partial \lambda_{C,3}}\right)^2 \sigma^2_{\lambda_{C,3}} + \left(\frac{\partial T_e}{\partial W_1}\right)^2 \sigma^2_{W_1} +$$
$$+ \left(\frac{\partial T_e}{\partial W_2}\right)^2 \sigma^2_{W_2} + \left(\frac{\partial T_e}{\partial W_3}\right)^2 \sigma^2_{W_3} + \sum_{j=1}^{m} \left(\frac{\partial T_e}{\partial \lambda_{0,1,j}}\right)^2 \sigma^2_{\lambda_{0,1,j}} + \sum_{j=1}^{m} \left(\frac{\partial T_e}{\partial \lambda_{0,2,j}}\right)^2 \sigma^2_{\lambda_{0,2,j}} +$$
$$+ \sum_{j=1}^{m} \left(\frac{\partial T_e}{\partial \lambda_{0,3,j}}\right)^2 \sigma^2_{\lambda_{0,3,j}} + \sum_{j=1}^{m} \left(\frac{\partial T_e}{\partial \sigma_{1,j}}\right)^2 \sigma^2_{\sigma_{1,j}} + \sum_{j=1}^{m} \left(\frac{\partial T_e}{\partial \sigma_{2,j}}\right)^2 \sigma^2_{\sigma_{2,j}} + \sum_{j=1}^{m} \left(\frac{\partial T_e}{\partial \sigma_{3,j}}\right)^2 \sigma^2_{\sigma_{3,j}} \tag{18}$$

Applying the uncertainties given in table 1 in equation (18), where each term is given in the appendix A, and taking into account that the uncertainty in the signal ratio σ_R is about 10%, the evaluated uncertainty in the electron temperature is given in table 2.

Table 2. Uncertainties in the electron temperature.

$P_{S,2}/P_{S,1}$	$\frac{\sigma_{T_e}}{T_e}$	$P_{S,3}/P_{S,1}$	$\frac{\sigma_{T_e}}{T_e}$	$(P_{S,3} + P_{S,2})/P_{S,1}$	$\frac{\sigma_{T_e}}{T_e}$
$(60 \pm 27) \cdot 10^1 eV$	45%	$600 \pm 99eV$	16.5%	$(60 \pm 12) \cdot 10^1 eV$	20%
$400 \pm 87eV$	22%	$400 \pm 41eV$	10%	$400 \pm 41eV$	10%
$200 \pm 21eV$	11%	$200 \pm 11eV$	11%	$200 \pm 10eV$	5%
$100 \pm 6eV$	6%	$100 \pm 4eV$	4%	$100 \pm 4eV$	4%

It is important to note that the uncertainty in the signal ratio σ_R that is related to the noise level in the signal depends on plasma density. For low density plasmas $n_e \simeq 1.10^{13} cm^{-3}$, the uncertainty σ_R can be of the order of 15%.

From table 2 it can be concluded that for high temperatures the best option to measure electron temperature from the signal ratio is $P_{S,3}/P_{S,1}$, which gives the smallest uncertainty in the electron temperature.

From table 2 it can be also concluded that for low plasma temperatures the uncertainty is lower. However, in TCABR the electron temperature is nowadays measured just in one spatial point at the plasma center, therefore for the plasma edge, where temperature maybe of order of $100eV$, plasma density is lower and consequently the uncertainty in electron temperature will be higher.

5. Conclusions

In this work a procedure to estimate the uncertainty in the electron temperature measured by the Thomson scattering diagnostic in TCABR has been presented. The results obtained with an analytic expression for the electron temperature as function of the signal ratio and other optical parameters of the polychromator show good agreement with results obtained directly from the computation of (1) and (2).

From figures 4 and 5 it can be concluded that the best option to evaluate the electron temperature is from the ratio of channel 2 plus channel 3 and channel 1 ($P_{S,3}/P_{S,1}$). However, error analysis shows that the uncertainty for this case is 5% higher.

Analysis of the uncertainties in electron temperature is dominated by uncertainties in parameter R, the signal ratio, which depends on noise in each channel. So the uncertainties in the filters and detector parameters have small influence on the electron temperature.

Acknowledgments

This work was partially supported by the Foundation for Supporting Research of the State of São Paulo (FAPESP projects 2010/50496-4 and 2011/50773-0), and FINEP (project 01.11.0092.00), Brazil.

Appendix A.

In this appendix each derivative in equation (18) is calculated. Firstly the case $R = P_{S,2}/P_{S,1}$ is calculated, and then the case $R = (P_{S,3} + P_{S,2})/P_{S,1}$ is calculated. For the case $R = P_{S,3}/P_{S,1}$ all indexes 2 must be changed to 3.

1) $R = P_{S,2}/P_{S,1}$:

Let

$$\gamma = \frac{\lambda_I^2 2k_B}{c^2 m_e}$$

$$\beta = \left(1 + K_1/\sqrt{K_1^2 - 4K_2K_0}\right)$$

$$\delta = \left(\frac{K_0}{K_2\sqrt{K_1^2 - 4K_2K_0}} + \frac{K_1 + \sqrt{K_1^2 - 4K_2K_0}}{2K_2^2}\right)$$

$$L_{C,n} = \lambda_{C,n} - \lambda_I$$

Then

$$\frac{\partial T_e}{\partial R} = -\gamma\beta\frac{W_1 b_1 W_2 b_2}{RK_2} \tag{1A}$$

$$\frac{\partial T_e}{\partial \lambda_{C,1}} = A_{\lambda_{C,1}} + B_{\lambda_{C,1}} + C_{\lambda_{C,1}} \tag{2A}$$

where:

$$A_{\lambda_{C,1}} = -\gamma\beta\frac{W_1W_2b_2}{K_2}\left[\ln\left(\frac{RW_1b_1}{W_2b_2}\right)+1\right]\sum_{j=1}^{3}\lambda_{0,1,j}$$

$$B_{\lambda_{C,1}} = -2\gamma^2\delta W_1a_2\sum_{j=1}^{3}\lambda_{0,1,j}$$

$$C_{\lambda_{C,1}} = \frac{W_1W_2b_2}{\sqrt{K_1^2-4K_2K_0}}\left[(L_{C,2}^2-L_{C,1}^2)\sum_{j=1}^{3}\lambda_{0,1,j}-2b_1L_{C,1}\right]$$

$$\frac{\partial T_e}{\partial\lambda_{C,2}} = A_{\lambda_{C,2}}+B_{\lambda_{C,2}}+C_{\lambda_{C,2}} \tag{3A}$$

where:

$$A_{\lambda_{C,2}} = -\gamma\beta\frac{W_1W_2b_1}{K_2}\left[\ln\left(\frac{RW_1b_1}{W_2b_2}\right)-1\right]\sum_{j=1}^{5}\lambda_{0,2,j}$$

$$B_{\lambda_{C,2}} = 2\gamma^2\delta W_2a_1\sum_{j=1}^{5}\lambda_{0,2,j}$$

$$C_{\lambda_{C,2}} = \frac{W_1W_2b_1}{\sqrt{K_1^2-4K_2K_0}}\left[(L_{C,2}^2-L_{C,1}^2)\sum_{j=1}^{5}\lambda_{0,2,j}+2b_2L_{C,2}\right]$$

$$\frac{\partial T_e}{\partial W_1} = A_{W_1}+B_{W_1}+C_{W_1} \tag{4A}$$

where:

$$A_{W_1} = -\gamma\beta\frac{W_2b_2}{K_2}\left[\ln\left(\frac{RW_1b_1}{W_2b_2}\right)+1\right]\left(b_1+\frac{W_1^2}{12}\right)$$

$$B_{W_1} = 2\gamma^2\delta a_2\left[-b_1-\frac{W_1^2}{12}+\frac{W_2b_2}{a_2}\right]$$

$$C_{W_1} = \frac{W_2b_2\left(L_{C,2}^2-L_{C,1}^2\right)}{\sqrt{K_1^2-4K_2K_0}}\left(b_1+\frac{W_1^2}{12}\right)$$

$$\frac{\partial T_e}{\partial W_2} = A_{W_2}+B_{W_2}+C_{W_2} \tag{5A}$$

where:

$$A_{W_2} = -\gamma\beta\frac{W_1b_1}{K_2}\left[\ln\left(\frac{RW_1b_1}{W_2b_2}\right)-1\right]\left(b_2+\frac{W_2^2}{12}\right)$$

$$B_{W_2} = 2\gamma^2\delta a_1\left[b_2+\frac{W_2^2}{12}-\frac{W_1b_1}{a_1}\right]$$

$$C_{W_2} = \frac{W_1b_1}{\sqrt{K_1^2-4K_2K_0}}\left[b_2+\frac{W_2^2}{12}\right]$$

$$\frac{\partial T_e}{\partial \lambda_{0,1,j}} = A_{\lambda_{0,1,j}} + B_{\lambda_{0,1,j}} + C_{\lambda_{0,1,j}} \tag{6A}$$

where:

$$A_{\lambda_{0,1,j}} = -\gamma\beta \frac{W_1 W_2 b_2}{K_2} \left[\ln\left(\frac{R W_1 b_1}{W_2 b_2} \right) + 1 \right] (L_{C,1} - \lambda_{0,1,j})$$
$$B_{\lambda_{0,1,j}} = -2\gamma^2 \delta \left[b_2 W_2 + a_2 W_1 (L_{C,1} - \lambda_{0,1,j}) \right]$$
$$C_{\lambda_{0,1,j}} = \frac{W_1 W_2 b_2 \left(L_{C,2}^2 - L_{C,1}^2 \right) (L_{C,1} - \lambda_{0,1,j})}{\sqrt{K_1^2 - 4K_2 K_0}}$$

$$\frac{\partial T_e}{\partial \lambda_{0,2,j}} = A_{\lambda_{0,2,j}} + B_{\lambda_{0,2,j}} + C_{\lambda_{0,2,j}} \tag{7A}$$

where:

$$A_{\lambda_{0,2,j}} = -\gamma\beta \frac{W_1 W_2 b_1}{K_2} \left[\ln\left(\frac{R W_1 b_1}{W_2 b_2} \right) - 1 \right] (L_{C,2} - \lambda_{0,2,j})$$
$$B_{\lambda_{0,2,j}} = 2\gamma^2 \delta \left[a_1 W_2 (L_{C,2} - \lambda_{0,2,j}) - W_1 b_1 \right]$$
$$C_{\lambda_{0,2,j}} = \frac{W_1 W_2 b_1 \left(L_{C,2}^2 - L_{C,1}^2 \right) (L_{C,2} - \lambda_{0,2,j})}{\sqrt{K_1^2 - 4K_2 K_0}}$$

$$\frac{\partial T_e}{\partial \sigma_{1,j}} = A_{\sigma_{1,j}} + B_{\sigma_{1,j}} + C_{\sigma_{1,j}} \tag{8A}$$

where:

$$A_{\sigma_{1,j}} = \gamma\beta\sigma_{1,j} \frac{W_1 W_2 b_2}{K_2} \left[\ln\left(\frac{R W_1 b_1}{W_2 b_2} \right) + 1 \right]$$
$$B_{\sigma_{1,j}} = 2\gamma^2 \delta \sigma_{1,j} W_1 a_2$$
$$C_{\sigma_{1,j}} = -\frac{\sigma_{1,j} W_1 W_2 b_2 \left(L_{C,2}^2 - L_{C,1}^2 \right)}{\sqrt{K_1^2 - 4K_2 K_0}}$$

$$\frac{\partial T_e}{\partial \sigma_{2,j}} = A_{\sigma_{2,j}} + B_{\sigma_{2,j}} + C_{\sigma_{2,j}} \tag{9A}$$

where:

$$A_{\sigma_{2,j}} = \gamma\beta\sigma_{2,j} \frac{W_1 W_2 b_1}{K_2} \left[\ln\left(\frac{R W_1 b_1}{W_2 b_2} \right) - 1 \right]$$

$$B_{\sigma_{2,j}} = -2\gamma^2 \delta \sigma_{2,j} W_2 a_1$$
$$C_{\sigma_{2,j}} = -\frac{\sigma_{2,j} W_1 W_2 b_1 \left(L_{C,2}^2 - L_{C,1}^2 \right)}{\sqrt{K_1^2 - 4K_2 K_0}}$$

2) $R = (P_{S,3} + P_{S,2})/P_{S,1}$:

$$\frac{\partial T_e}{\partial R} = -\gamma\beta \frac{W_1 b_1 (W_2 b_2 + W_3 b_3)}{R K_2} \tag{10A}$$

$$\frac{\partial T_e}{\partial \lambda_{C,1}} = A_{\lambda_{C,1}} + B_{\lambda_{C,1}} + C_{\lambda_{C,1}} \tag{11A}$$

where:

$$A_{\lambda_{C,1}} = -\gamma\beta \frac{W_1 (W_2 b_2 + W_3 b_3)}{K_2} \left[\ln\left(\frac{R W_1 b_1}{W_2 b_2 + W_3 b_3} \right) + 1 \right] \sum_{j=1}^{3} \lambda_{0,1,j}$$

$$B_{\lambda_{C,1}} = -2\gamma^2 \delta W_1 (a_2 + a_3) \sum_{j=1}^{3} \lambda_{0,1,j}$$

$$C_{\lambda_{C,1}} = \frac{W_1 (W_2 b_2 + W_3 b_3)}{\sqrt{K_1^2 - 4 K_2 K_0}} \left[(L_{CM}^2 - L_{C,1}^2) \sum_{j=1}^{3} \lambda_{0,1,j} + 2 b_1 L_{C,1} \right]$$

$$\frac{\partial T_e}{\partial \lambda_{C,2}} = A_{\lambda_{C,2}} + B_{\lambda_{C,2}} + C_{\lambda_{C,2}} \tag{12A}$$

where:

$$A_{\lambda_{C,2}} = -\gamma\beta \frac{W_1 W_2 b_1}{K_2} \left[\ln\left(\frac{R W_1 b_1}{W_2 b_2 + W_3 b_3} \right) - 1 \right] \sum_{j=1}^{5} \lambda_{0,2,j}$$

$$B_{\lambda_{C,2}} = 2\gamma^2 \delta W_2 a_1 \sum_{j=1}^{5} \lambda_{0,2,j}$$

$$C_{\lambda_{C,2}} = \frac{W_1 W_2 b_1}{\sqrt{K_1^2 - 4 K_2 K_0}} \left[(L_{CM}^2 - L_{C,1}^2) \sum_{j=1}^{5} \lambda_{0,2,j} + 2 \frac{(W_2 b_2 + W_3 b_3)}{W_2 + W_3} L_{CM} \right]$$

$$\frac{\partial T_e}{\partial \lambda_{C,3}} = A_{\lambda_{C,3}} + B_{\lambda_{C,3}} + C_{\lambda_{C,3}} \tag{13A}$$

where:

$$A_{\lambda_{C,3}} = -\gamma\beta \frac{W_1 W_3 b_1}{K_2} \left[\ln\left(\frac{R W_1 b_1}{W_2 b_2 + W_3 b_3} \right) - 1 \right] \sum_{j=1}^{7} \lambda_{0,3,j}$$

$$B_{\lambda_{C,3}} = 2\gamma^2 \delta W_3 a_1 \sum_{j=1}^{7} \lambda_{0,3,j}$$

$$C_{\lambda_{C,3}} = \frac{W_1 W_3 a_1}{\sqrt{K_1^2 - 4 K_2 K_0}} \left[(L_{CM}^2 - L_{C,1}^2) \sum_{j=1}^{7} \lambda_{0,3,j} + 2 \frac{(W_2 b_2 + W_3 b_3)}{W_2 + W_3} L_{CM} \right]$$

$$\frac{\partial T_e}{\partial W_1} = A_{W_1} + B_{W_1} + C_{W_1} \tag{14A}$$

where:

$$A_{W_1} = -\gamma\beta\frac{(W_2b_2 + W_3b_3)}{K_2}\left[\ln\left(\frac{RW_1b_1}{W_2b_2 + W_3b_3}\right) + 1\right]\left(b_1 + \frac{W_1^2}{12}\right)$$

$$B_{W_1} = 2\gamma^2\delta\left(a_2 + a_3\right)\left[-b_1 - \frac{W_1^2}{12} + \frac{(W_2b_2 + W_3b_3)}{a_2 + a_3}\right]$$

$$C_{W_1} = \frac{(W_2b_2 + W_3b_3)\left(L_{CM}^2 - L_{C,1}^2\right)}{\sqrt{K_1^2 - 4K_2K_0}}\left(b_1 + \frac{W_1^2}{12}\right)$$

$$\frac{\partial T_e}{\partial W_2} = A_{W_2} + B_{W_2} + C_{W_2} \tag{15A}$$

where:

$$A_{W_2} = -\gamma\beta\frac{W_1b_1}{K_2}\left[\ln\left(\frac{RW_1b_1}{W_2b_2 + W_3b_3}\right) - 1\right]\left(b_2 + \frac{W_2^2}{12}\right)$$

$$B_{W_2} = 2\gamma^2\delta a_1\left[b_2 + \frac{W_2^2}{12} - \frac{W_1b_1}{a_1}\right]$$

$$C_{W_2} = \frac{W_1b_1\left(L_{CM}^2 - L_{C,1}^2\right)}{\sqrt{K_1^2 - 4K_2K_0}}\left[b_2 + \frac{W_2^2}{12} + 2W_3L_{CM}\frac{(W_2b_2 + W_3b_3)\left(\lambda_{C,2} - \lambda_{C,3}\right)}{\left(L_{CM}^2 - L_{C,1}^2\right)\left(W_2 + W_3\right)^2}\right]$$

$$\frac{\partial T_e}{\partial W_3} = A_{W_3} + B_{W_3} + C_{W_3} \tag{16A}$$

where:

$$A_{W_3} = -\gamma\beta\frac{W_1b_1}{K_2}\left[\ln\left(\frac{RW_1b_1}{W_2b_2 + W_3b_3}\right) - 1\right]\left(b_3 + \frac{W_3^2}{12}\right)$$

$$B_{W_3} = 2\gamma^2\delta a_1\left[b_3 + \frac{W_3^2}{12} - \frac{W_1b_1}{a_1}\right]$$

$$C_{W_3} = \frac{W_1b_1\left(L_{CM}^2 - L_{C,1}^2\right)}{\sqrt{K_1^2 - 4K_2K_0}}\left[b_3 + \frac{W_3^2}{12} + 2W_2L_{CM}\frac{(W_2b_2 + W_3b_3)\left(\lambda_{C,3} - \lambda_{C,2}\right)}{\left(L_{CM}^2 - L_{C,1}^2\right)\left(W_2 + W_3\right)^2}\right]$$

$$\frac{\partial T_e}{\partial \lambda_{0,1,j}} = A_{\lambda_{0,1,j}} + B_{\lambda_{0,1,j}} + C_{\lambda_{0,1,j}} \tag{17A}$$

where:

$$A_{\lambda_{0,1,j}} = -\gamma\beta\frac{W_1\left(W_2b_2 + W_3b_3\right)}{K_2}\left[\ln\left(\frac{RW_1b_1}{W_2b_2 + W_3b_3}\right) + 1\right]\left(L_{C,1} - \lambda_{0,1,j}\right)$$

$$B_{\lambda_{0,1,j}} = -2\gamma^2\delta\left[W_1\left(a_2 + a_3\right)\left(L_{C,1} - \lambda_{0,1,j}\right) + \left(W_2b_2 + W_3b_3\right)\right]$$

$$C_{\lambda_{0,1,j}} = \frac{W_1\left(W_2b_2 + W_3b_3\right)\left(L_{CM}^2 - L_{C,1}^2\right)\left(L_{C,1} - \lambda_{0,1,j}\right)}{\sqrt{K_1^2 - 4K_2K_0}}$$

$$\frac{\partial T_e}{\partial \lambda_{0,2,j}} = A_{\lambda_{0,2,j}} + B_{\lambda_{0,2,j}} + C_{\lambda_{0,2,j}} \tag{18A}$$

where:

$$A_{\lambda_{0,2,j}} = -\gamma\beta \frac{W_1 W_2 b_1}{K_2} \left[\ln\left(\frac{R W_1 b_1}{W_2 b_2 + W_3 b_3} \right) - 1 \right] (L_{C,2} - \lambda_{0,2,j})$$
$$B_{\lambda_{0,2,j}} = 2\gamma^2 \delta \left[a_1 W_2 \left(L_{C,2} - \lambda_{0,2,j} \right) + W_1 b_1 \right]$$
$$C_{\lambda_{0,2,j}} = \frac{W_1 W_2 b_1 \left(L_{CM}^2 - L_{C,1}^2 \right) (L_{C,2} - \lambda_{0,2,j})}{\sqrt{K_1^2 - 4K_2 K_0}}$$

$$\frac{\partial T_e}{\partial \lambda_{0,3,j}} = A_{\lambda_{0,3,j}} + B_{\lambda_{0,3,j}} + C_{\lambda_{0,3,j}} \tag{19A}$$

where:

$$A_{\lambda_{0,3,j}} = -\gamma\beta \frac{W_1 W_3 b_1}{K_2} \left[\ln\left(\frac{R W_1 b_1}{W_2 b_2 + W_3 b_3} \right) - 1 \right] (L_{C,3} - \lambda_{0,3,j})$$
$$B_{\lambda_{0,3,j}} = 2\gamma^2 \delta \left[a_1 W_3 \left(L_{C,3} - \lambda_{0,3,j} \right) + W_1 b_1 \right]$$
$$C_{\lambda_{0,3,j}} = \frac{W_1 W_3 b_1 \left(L_{CM}^2 - L_{C,1}^2 \right) (L_{C,3} - \lambda_{0,3,j})}{\sqrt{K_1^2 - 4K_2 K_0}}$$

$$\frac{\partial T_e}{\partial \sigma_{1,j}} = A_{\sigma_{1,j}} + B_{\sigma_{1,j}} + C_{\sigma_{1,j}} \tag{20A}$$

where:

$$A_{\sigma_{1,j}} = \gamma\beta\sigma_{1,j} W_1 \frac{(W_2 b_2 + W_3 b_3)}{K_2} \left[\ln\left(\frac{R W_1 b_1}{W_2 b_2 + W_3 b_3} \right) + 1 \right]$$
$$B_{\sigma_{1,j}} = 2\gamma^2 \delta \sigma_{1,j} \left(a_2 + a_3 \right)$$
$$C_{\sigma_{1,j}} = -\frac{\sigma_{1,j} W_1 \left(W_2 b_2 + W_3 b_3 \right) \left(L_{CM}^2 - L_{C,1}^2 \right)}{\sqrt{K_1^2 - 4K_2 K_0}}$$

$$\frac{\partial T_e}{\partial \sigma_{2,j}} = A_{\sigma_{2,j}} + B_{\sigma_{2,j}} + C_{\sigma_{2,j}} \tag{21A}$$

where:

$$A_{\sigma_{2,j}} = \gamma\beta\sigma_{2,j} \frac{W_1 W_2 b_1}{K_2} \left[\ln\left(\frac{R W_1 b_1}{W_2 b_2 + W_3 b_3} \right) - 1 \right]$$
$$B_{\sigma_{2,j}} = -2\gamma^2 \delta \sigma_{2,j} W_2 a_1$$
$$C_{\sigma_{2,j}} = -\frac{\sigma_{2,j} W_1 W_2 b_1 \left(L_{CM}^2 - L_{C,1}^2 \right)}{\sqrt{K_1^2 - 4K_2 K_0}}$$

$$\frac{\partial T_e}{\partial \sigma_{3,j}} = A_{\sigma_{3,j}} + B_{\sigma_{3,j}} + C_{\sigma_{3,j}} \tag{22A}$$

where:

$$A_{\sigma_{3,j}} = \gamma\beta\sigma_{3,j}\frac{W_1W_3b_1}{K_2}\left[\ln\left(\frac{RW_1b_1}{W_2b_2+W_3b_3}\right)-1\right]$$
$$B_{\sigma_{3,j}} = -2\gamma^2\delta\sigma_{3,j}W_3a_1$$
$$C_{\sigma_{3,j}} = -\frac{\sigma_{3,j}W_1W_3b_1\left(L_{CM}^2-L_{C,1}^2\right)}{\sqrt{K_1^2-4K_2K_0}}$$

References

[1] Ruchko L F et al 2002 *Braz. J. Phys.* **32(1)** 57-64
[2] Nascimento I C et al 2005 *Nucl. Fusion* **45** 796
[3] Nascimento I C et al 2007 *Nucl. Fusion***47** 1570
[4] Severo J H F Tsypin V S, Galvão R M O, Nascimento I C, Tendler M and Fagundes A N 2002 *Braz. J. Phys* **32(1)** 13-9
[5] Severo J H F, Nascimento I C, Tsypin V S and Galvão R M O 2003 *Nucl. Fusion* **43** 1047-1056
[6] Severo J H F et al 2009 *Nucl. Fusion* **49** 115026
[7] Severo J H F, Nascimento I C, Tsypin V S, Kuznetov Yu K, Saettone E A, Vannucci A, Galvão R M O, Tendler M and Mikhailovskii A B 2004 *Phys. Plasma* **11(2)** 846-848
[8] Alonso M P, Figueiredo A C A, Borges F O, Elizondo J I, Galvão R M O, Severo J H F, Usuriaga O C, Berni L A and Machida M 2010 *Rev. Sci. Inst.* **81** 10D529
[9] Severo J H F, Nascimento I C, Kuznetov Yu K, Tsypin V S, Galvão R M O and Tendler M 2007 *Rev. Sci Inst.* **78** 043509
[10] Alonso M P et al 2010 *J. Phys.: Conf. Series* **227** 012027
[11] Forrest, M J, Peacock N J, Robinson D C, Sannikov V V and Wilcock P D 1970 *Culham Plasma Physics Laboratory Report CLM-R 107* (Abingdon)
[12] Anashin A M, Gorbunov E P, Ivanov D P, Lysenko S E, Peacock N J, Robinson D C, Sannikov V V and Strelkov V S 1971 *Sov. Phys. - JETP* **33** 1127
[13] Rautian S G 1958 *Sov. Phys. Uspekhi* **66(1)** 245
[14] Alonso M P, Figueiredo A C A, Berni L A, Varandas C A F 2008 *IEEE Trans. Plasma Sci.* **36(4)** 1094
[15] Sheffield J 1975 *Plasma Scattering of Electromagnetic Radiation* (New York: Academic press)